IUPAC International Union of Pure and Applied Chemistry

REPRINTED FROM

Handbook of Thermodynamic and Transport Properties of Alkali Metals

ISBN 0-632-01447-4

EDITOR
Roland W. Ohse

Blackwell Scientific Publications · 1985

CHAPTER 3.6

MAGNETOHYDRODYNAMIC POWER GENERATION, ELECTROMAGNETIC PUMPS, HEAT PIPES, AND THERMIONIC CONVERTORS

E. S. Pierson[1], K. A. Bonyhady[2], P. F. Dunn[3],
R. D. Nathenson[4], and K. L. Uherka[3]

1. Purdue University, Calumet, Hammond, Indiana 46323
2. Ret. Staff Consulting Engineer, Rockwell Int'l. Co., Atomics Int'l. Div., Canoga Park, California 91304
3. Argonne National Laboratory, Argonne, Illinois 60439
4. Westinghouse Electric Corporation, Research & Development Center, Pittsburgh, Pennsylvania 15235

Contents

3.6.1 Magnetohydrodynamic Power Generation

INTRODUCTION

Magnetohydrodynamic (MHD) power generation was proposed in the late 1950's as a more efficient method of generating electric power (Ref. 1). In an MHD generator, indicated schematically in Fig. 1, an electrically conducting fluid flows with a velocity $\vec{U}$ across a magnetic field $\vec{B}$, creating a $\vec{U}x\vec{B}$ induced voltage (electromotive force) and a current density $\vec{J}=\sigma(\vec{E} + \vec{U}x\vec{B})$, where $\vec{E}$ is the electric field due to the voltage difference between the electrodes and σ is the (electrical) conductivity of the fluid. The $\vec{J}x\vec{B}$ force opposes the fluid motion and completes the energy-conversion process. Since this generator has no solid moving parts, higher temperatures (higher cycle efficiencies) than alternative schemes are possible.

Two types of MHD power generation are presently under investigation -- liquid metal and plasma. In the former the electrical conductivity is provided by a liquid metal, in the latter by a hot, ionized gas. MHD research is world-wide, with major active programs in Australia, China, India, Japan, the Netherlands, the United States, and the Union of Soviet Socialist Republics (Refs. 2-4). Both concepts are described below. The emphasis is on the former as it is a heavy user of alkali metal technology, although the latter is currently receiving more attention and financial support.

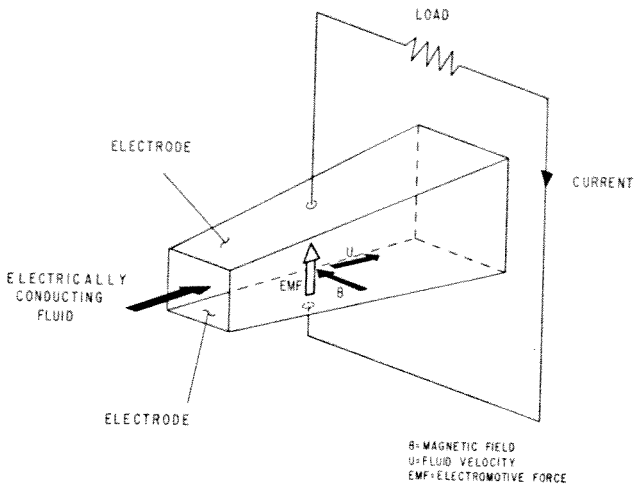

Fig. 1 Principle of the MHD Generator

LIQUID-METAL MAGNETOHYDRODYNAMICS

Cycles

The two-phase-generator liquid-metal MHD (LMMHD) cycles use two working fluids, a thermodynamic fluid (gas or vapor) and an electrodynamic fluid (liquid metal) to provide the electrical conductivity in the LMMHD generator. The two working fluids give LMMHD great versatility in coupling to different heat sources and operating over different temperature ranges. The cycle configurations currently under investigation are: 1) the Rankine-cycle version best suited to heat-source temperatures of 370 K to ~850 K (Ref. 5), 2) the Brayton-cycle version best suited to heat-source temperatures above ~730 K (Ref. 6), and 3) the open-cycle version for coal or other fossil fuels (Ref. 7).

The Brayton-cycle (gas-cycle) LMMHD concept schematic diagram with a gas turbine is shown in Fig. 2. An inert gas, e.g., helium, is the thermodynamic working fluid, and a liquid metal, e.g., sodium or lithium, is the electrodynamic fluid in the MHD generator. In operation, the gas and liquid are combined in the mixer and the resulting two-phase mixture enters the MHD generator. The MHD generator acts as a combined turbine and electric generator; the gas expands, drives the liquid across the magnetic field, and, thus, generates electrical power. Because the liquid has a high heat (energy) content, expansion occurs at almost constant temperature, and a great deal of energy is still available in the gas that leaves the MHD generator. (The liquid acts as an "infinite-reheat" source for the gas, heat energy is continuously transferred from the liquid to the gas, and most of the energy out of the generator comes from the liquid.) It is this almost-constant-temperature expansion that accounts for the potentially higher efficiency of the two-phase LMMHD concepts. From the MHD generator, the two-phase mixture enters a nozzle, where additional gas-liquid energy is used (as in the generator) to accelerate the liquid; the resulting high-speed flow is separated in a separator (possibly rotating to minimize losses), and the liquid pressure needed to return the liquid through the primary heat exchanger to the mixer is obtained in the diffuser. The nozzle-diffuser system may be replaced by a liquid-metal pump if better performance results.

The gas leaving the separator still has considerable thermal energy, which must be used effectively in order to obtain the highest efficiency for the system. It can be transferred from the hot gas to the colder gas in a regenerator, extracted with a gas turbine, extracted with a steam boiler (which would replace both the gas turbine and regenerator of Fig. 2), or used to provide heat for some other process in what is termed "cogeneration." These components can be combined.

Heat addition can be to the liquid metal, the gas, or both. Because the liquid-metal mass flow rate is much higher than the gas mass flow rate the heat addition can be solely to the liquid metal, with the gas being heated by the liquid in the mixer, to yield a simpler system without a significant effect on plant efficiency.

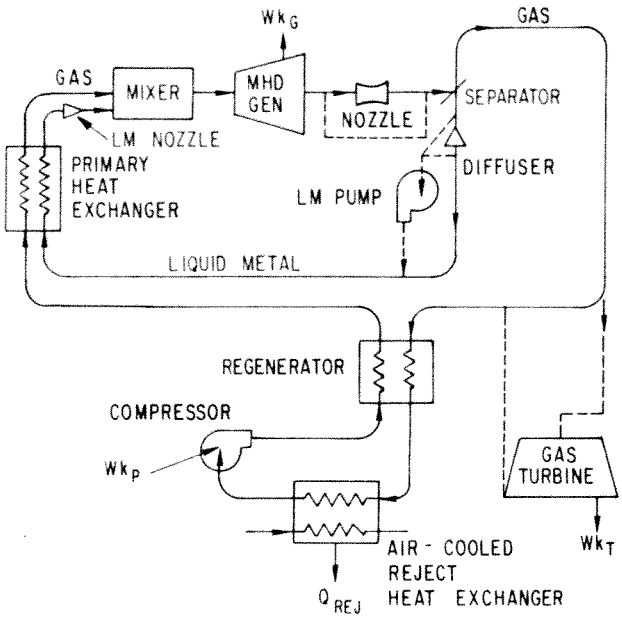

Fig. 2 The Brayton-cycle LMMHD Concept

The Rankine-cycle (vapor-cycle) LMMHD concept differs from the Brayton-cycle version only in the use of a condensable fluid, e.g., steam or neohexane, as the thermodynamic working fluid with a compatible liquid metal, e.g., tin or NaK. Again, the energy in the (superheated) vapor leaving the separator is recovered in a regenerator, a low-pressure turbine, or used for process heat, and heat addition can be solely to the liquid metal, with the vapor being generated from the condensate in a direct-contact mixing boiler. Because of the almost-constant-temperature expansion, LMMHD Rankine-cycle calculated efficiencies are higher than those of conventional plants for the same source and sink temperatures. The LMMHD Rankine cycle is also under consideration for high-temperature space power systems with, for example, cesium as the vapor and lithium as the liquid metal (Ref. 8). Temperatures would be above 900 K.

The open-cycle version differs from the Brayton-cycle version in using an open rather than a closed gas cycle. Combustion gas (from coal or other fossil fuels) is used as the thermodynamic fluid with a compatible liquid metal, most likely copper or a copper alloy, thereby eliminating the need for a primary heat exchanger. Coal is burned with air in a pressurized, vortex-type combustor (similar to a conventional cyclone furnace). The combustion products go from the combustor to the LMMHD mixer, where they are mixed with the liquid metal; thus, the liquid is heated by the combustion gas in the mixer. The two-phase and pure-liquid-metal components are the same as for the other versions. Leaving the LMMHD loop, the energy remaining in the combustion gas is used in a conventional boiler plant, a gas turbine, or a process heat application.

Components

The two-phase LMMHD generator is the key component in the cycle, and the most unusual. It inherently has a high efficiency if the loss mechanisms not basic to its operation replace by viscous losses and slip losses can be controlled. Thus, research has focused on studiesof the individual losses, studies of two-phase flows in a magnetic field, and generator models and experiments as described below:

(1) End losses i.e., ohmic losses due to current reversal in the generator end regions as a result of spatially decreasing magnetic fields, set a lower limit to the generator's length and an upper limit to the generator's voltage. Early work established the use of insulating vanes (Ref. 9) and multiple generators (Ref. 10) to minimize end currents and losses. A numerical model allows the calculation of the end loss for an arbitrary arrangement of insulating vanes (number, lengths, locations) (Ref. 11).

(2) Viscous losses (due to wall shear) are small because the electromagnetic forces are so much larger than all other forces. However, wall shear causes a pure-liquid shunt layer adjacent to the wall with a low velocity. Current reversal occurs in this layer, and the effect of the current reversal is magnified because the liquid conductivity is higher than the two-phase core flow conductivity. Analysis has shown this effect to be very small (Ref. 12).

(3) Slip, where the gas velocity is higher than the liquid velocity, reduces the efficiency of the generator and the cycle. The most-recent data clearly shows that at higher electromagnetic interactions the slip loss is small (Ref. 13).

To better understand LMMHD generators, basic studies have been made. These have included experiments focused on single- and two-phase flows in the generator (Ref. 14), the electrical conductivity of two-phase mixtures (Ref. 15), and the slip under different conditions (Ref. 16).

The impact of the above work on generator efficiency is dramatically demonstrated by the data of Fig. 3 (Ref. 13). The efficiency has increased with experience, and for the most recent channel (LT-4) is substantially higher at high void fractions. The power density is comparable to or above that anticipated for commercial generators, thus minimizing the chances of encountering unanticipated problems in scaling to larger generators. Efficiencies in excess of 0.60 were obtained with a small generator [~20 kW(e)] which had no provision (such as vanes) to minimize end losses.

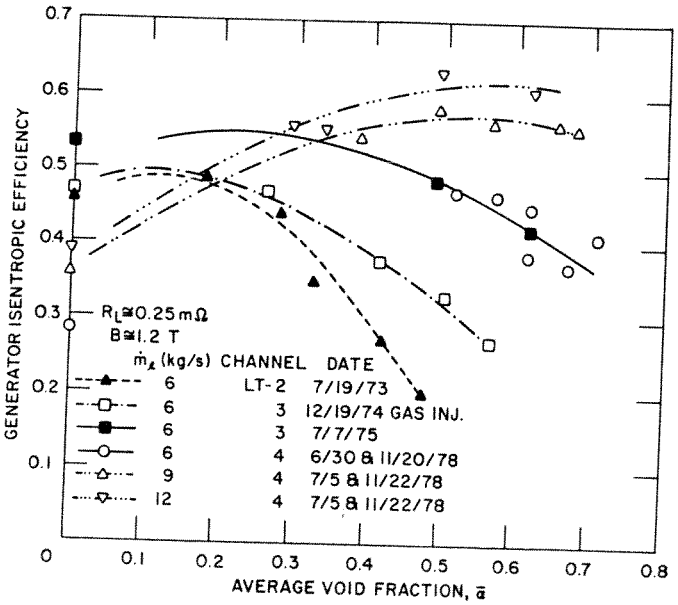

Fig. 3 LMMHD Generator Efficiency versus Void Fraction

There is a substantial body of two-phase literature, much of which is applicable to mixers, nozzles, diffusers, and separators for LMMHD systems. Experiments have established mixer characteristics under various operating conditions (Refs. 17,18), and the results indicate that element and contraction-geometry designs are the most critical factors. Both two-component, two-phase and one-component, two-phase nozzles have been studied, as well as two-phase diffusers (Ref. 19).

High-performance gas-liquid separators have been investigated for many applications. For flat-plate separators, excellent agreement was obtained between the test results and model (Ref. 19). A novel impinging-jet separator showed significant liquid concentration (>3 to 1) is possible with very low velocity losses (Ref. 19). Rotating separators, which minimize the viscous loss, are very attractive. Biphase Energy Systems has considerable experimental experience, including field tests, with rotary separator turbines for generating power from geothermal brines (Ref. 20).

Typical Applications

LMMHD energy-conversion systems have been studied in connection with many heat or energy sources. The significant features of LMMHD coupled to nuclear and solar energies are summarized here. The open-cycle system with coal is not covered since alkali metals are not used.

The reasons for considering LMMHD for liquid-metal-cooled fast breeder reactors (LMFBRs) and controlled thermonuclear reactors (CTRs) are: 1) energy-conversion systems without water will eliminate any potentially-hazardous water-liquid metal interface; 2) potential containment material problems are minimized by using the same liquid metal (sodium or lithium) in both the heat source and the energy conversion system, and 3) attractive conversion efficiencies are obtained, including the ability to utilize the higher temperatures associated with thermonuclear reactors. In addition, the LMMHD system may decrease the sensitivity to thermal transients (Ref. 5), and allow nuclear cogeneration systems with the process heat available at temperatures close to that of the heat source.

Recently, LMMHD applications with solar collectors have been considered in France, Israel, and the United States (Refs. 21,22). The reasons solar LMMHD appears attractive are: 1) the potential for a conversion efficiency higher than alternative conversion systems, or both electricity and high-temperature process heat (cogeneration); 2) the efficiency and cost are almost independent of size; and 3) the use of liquid-metal-cooled collectors means higher solar collector and/or conversion system efficiencies.

Performance (efficiency) studies for solar LMMHD applications have shown (Refs. 21-24): 1) the LMMHD Rankine cycle has a higher efficiency than other Rankine cycles without process heat, or the same efficiency with process heat as the other cycles have without process heat; and 2) the LMMHD Brayton cycle has an efficiency comparable to or higher than advanced Stirling engines, and is very attractive for cogeneration applications. Cost studies have also demonstrated clear economic advantages (Ref. 24).

AC MHD Generators

Most power applications either use ac (alternating current) directly, or use ac as an intermediate step to obtain the correct dc (direct current) characteristics. Thus, a number of ac MHD generator schemes have been investigated. The most important are induction, conduction, and slug. None are currently under investigation because the efficiencies are lower than for dc generators, and because high-efficiency dc-to-ac conversion equipment is now available (Ref. 7).

The induction generator, a linear induction machine with a conducting liquid as the moving secondary (Refs. 25,26), is a direct descendent of liquid-metal induction pumps (see Section 3.6.2) and rotating induction motors. In operation, a traveling electromagnetic field is produced by a stationary polyphase winding, Fig. 4. This field induces a current in the fluid with a magnitude proportional to the slip $s = (U_s - U)/U_s$ and the magnetic Reynolds number $R_m = \mu\sigma U_s \lambda/2\pi$, where U_s and U are the velocities of the traveling field and fluid, μ and σ are the permeability and conductivity of the fluid, and λ is the wavelength of the traveling field. If either s or R_m is zero, there is no induced current. There is no direct electrical connection to the fluid, so that the generated power is due to the change in the electrical impedance of the stationary winding.

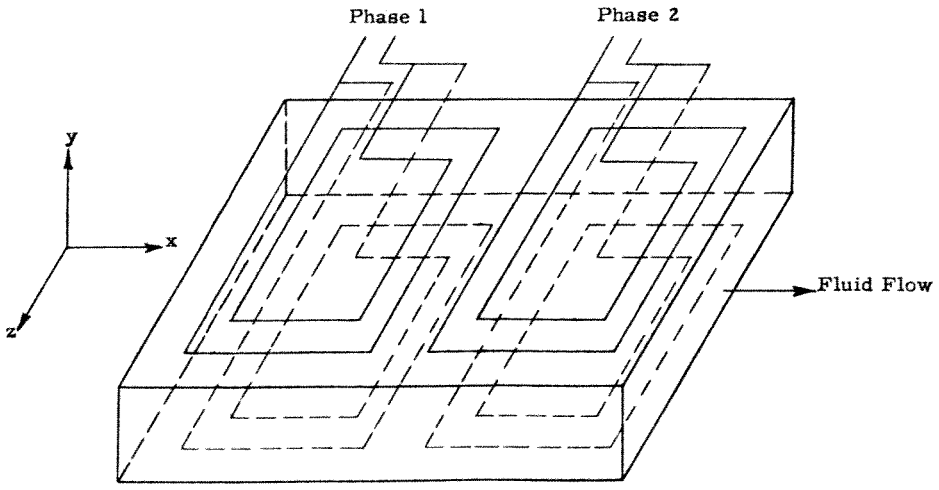

Fig. 4 Flat Linear MHD Induction Machine

Induction generators have been proposed for plasma MHD generators, but the electrical conductivity of a plasma is much too low to be practical (Ref. 25). With pure liquid metals the conductivity is acceptable (Ref. 25), but there is no LMMHD energy-conversion cycle currently under investigation which produces such a flow for the generator. With a two-phase flow the conductivity is marginally too low, and this approach is not being pursued.

AC conduction generators are the same as dc conduction generators except for an ac (sinusoidal) applied magnetic field which generates an ac voltage (and current). The power density is equal to that for the dc version if both have the same effective (heating) magnetic flux density and the inductive effects in the generator are negligible. Application is limited because of the large losses and high reactive power required for the ac magnet, and the fluctuating electromagnetic force.

The slug-flow generator uses alternating slugs of liquid metal and gas (or variable conductivity for a plasma MHD generator) to generate ac. There are two types -- conduction and parametric. In the conduction version an output current is produced only when a conducting slug is between the electrodes, so that the output waveform consists of a dc and an ac component. This type of output waveform requires separate processing of the dc and ac components.

A unidirectional slug flow generator can produce pure ac if the electrodes on each side of the channel are segmented and connected to alternating sides of a transformer (Ref. 27). However, considerable shorting through the slugs and a liquid layer on the electrodes could be limiting factors. AC can also be produced by an oscillating slug without shorting problems (Ref. 28). The slug-flow generator schemes have not received attention lately, primarily because of limitations inherent in the thermodynamic cycles which produce the slugs.

In the parametric version the conducting slug changes the magnetic flux linking a coil as it flows through the coil, thus generating ac power (much as in a rotating reluctance generator) (Ref. 27). Unfortunately, the interaction is not strong and the reactive power requirements are large.

PLASMA MAGNETOHYDRODYNAMICS

Cycles

Several MHD power generation systems use an ionized gas, i.e., a plasma, as the working fluid. In the generators of these systems, plasma electrical conductivities on the order of 10 S/m can be achieved, as compared to $\sim 10^6$ S/m for liquid metals. Yet, power densities comparable to or slightly less than those of liquid-metal MHD generators ($\sim$10 MW/m^3) can be obtained, primarily because the plasma velocity is roughly two orders of magnitude greater than the liquid-metal velocity.

The plasma attains an electrical conductivity sufficient for power generation through ionization. This is accomplished by "seeding" the plasma with an alkali metal of low ionization potential e.g., cesium or potassium. When the seeded plasma is heated to very high temperatures ($\gtrsim$ 2800 K), electrical conductivities $\gtrsim$ 5 S/m are obtained (Refs. 4,30). This process is called thermal ionization. Conductivities of this magnitude also may be reached at lower temperatures ($\sim$ 1800 K) by nonequilibrium ionization. This is achieved through application of a strong magnetic field or some form of radiation which excites the plasma's electrons to higher temperatures than that of its ions (Ref. 31).

Specific MHD power generation systems have evolved that exploit each of the aforementioned ionization processes (Refs. 4,30). In an open-cycle plasma MHD system (OCMHD), the working fluid is thermally ionized by the high temperature ($\sim$2800 K) combustion of a fossil fuel burned with preheated air. Oxygen enrichment may be used to reduce the required oxidizer preheat temperature. Potassium is the "seed". In a closed-cycle plasma MHD system (CCMHD), the working fluid is a noble gas, such as argon, seeded with cesium. The noble gas is heated by a regenerative heat exchanger array to $\sim$ 1800 K by the combustion products of a fossil fuel and oxidant, or a heat source such as a nuclear reactor. Sufficient conductivity of the resultant plasma is obtained through nonequilibrium ionization.

The OCMHD and CCMHD systems differ principally in how the working fluid is coupled to the heat source and whether the working fluid goes through an open or a closed cycle. Both are most efficient when the MHD power generation components operate as the initial, or topping, stage of a combined cycle system. Most often, the MHD system is coupled to a steam power plant. The plasma working fluid follows an open Brayton cycle. In most cases, coal serves as the fossil fuel. The OCMHD system has been evaluated as a topping cycle for both Rankine and Brayton bottoming cycles. The coal-fired OCMHD coupled to a steam bottoming plant is envisioned to reach commercialization first, and to operate at a 45-50% overall efficiency.

The performance of the MHD generators in both plasma systems is characterized primarily by the isentropic efficiency and enthalpy extraction of the generator. Enthalpy extraction is a measure of how much thermal energy of the conducting fluid is converted into electrical energy. Isentropic efficiency is a measure of how much actual work (ultimately in the form of electrical power) is extracted from the generator versus the work that would be available if the gas expanded isentropically through the generator under the same pressure ratio. To achieve adequate performance, the generator must operate with a 70 to 80 percent isentropic efficiency and 20 percent enthalpy extraction. Typical values required of an OCMHD generator to achieve 20 percent enthalpy extraction from a 20-m long generator are an electrical conductivity of 8 S/m at a Mach number of 0.8 and an applied magnetic flux density of 8 T.

Components

The critical components of the OCMHD and CCMHD systems are the coal combustor, magnet, MHD generator, heat exchangers (including preheaters), and the seed-recovery and power-conditioning systems. Although both systems use similar components, they differ in design as dictated by the differences in the cycles (Refs. 4,30).

CCMHD employs a two-flow-path system (Fig. 5), with the first path open. Coal is combusted with preheated air to 1800-2000 K. The hot combustion gases flow through a refractory-lined regenerative heat exchanger array to heat the MHD working fluid to operating temperatures. The combustion gases then are directed through a combustion gas-to-air heat exchanger to the stack, where they are exhausted to the atmosphere. The transfer of heat from the combustion gas to the MHD plasma is accomplished cyclicly. The regenerative heat exchanger is heated first by the combustion gas, then the combustion gas is evacuated and the high-pressure noble gas introduced. Finally, any residual noble gas is purged from the heat exchanger and the reheat phase is begun again. The entire heat-exchanger array is operated such that thermal energy is transferred to the MHD fluid continuously. Once heated, the inert gas is seeded with cesium and accelerated through a nozzle into the MHD generator. After exiting the generator, it passes through the steam boiler and the precooler, and is compressed and returned to the heat-exchanger array. The cesium is removed in the steam boiler and inert gas precooler, purified, and then reinjected into the hot inert gas.

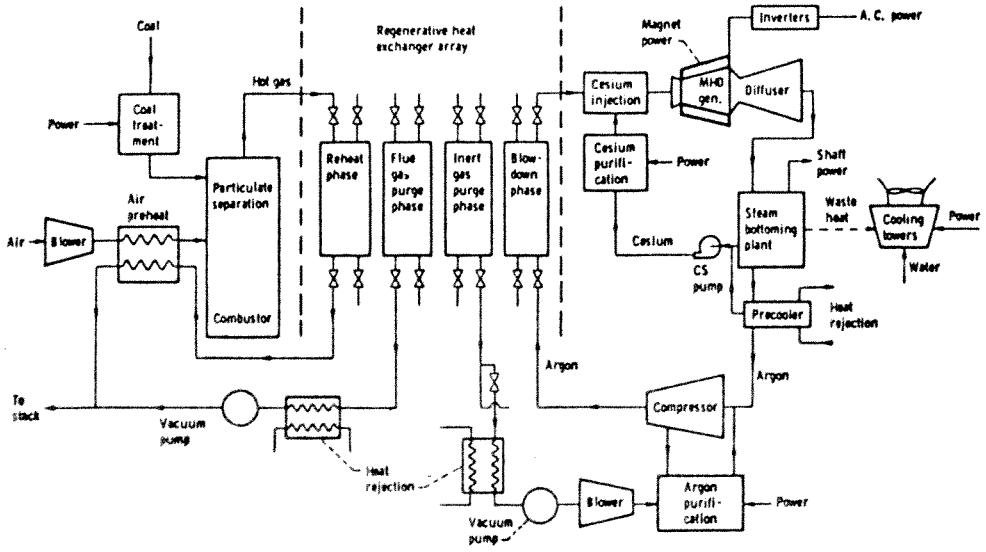

Fig. 5 CCMHD Topping Cycle

OCMHD uses a single-flow-path system, Fig. 6, and the seeded hot combustion gases are used directly as the MHD working fluid. The coal-fired OCMHD power plant is comprised of an MHD topping unit and a steam bottoming system. In the primary combustor of the topping unit, preheated, compressed air and coal are burned under pressure at temperatures as high as 3000 K. The combustion is fuel-rich to limit the amount of NO produced. Potassium salts are added in the combustor as seed material. The combustion mixture passes through the MHD channel to generate electrical power, the diffuser to recover kinetic energy, and then into the steam bottoming system. Like the steam generation system in a conventional power plant,

the bottoming system has the primary functions of efficiently extracting heat from the combustion gas to produce high-pressure steam and to preheat combustion air, and of controlling the emission of pollutants such as NO_x, SO_x, CO, and particulates. In addition, this system must recover a large fraction of the seed material and complete the combustion of the fuel-rich gas. Sufficient gas residence time (1-3 ms) is allowed in the radiant boiler for NO relaxation to occur. Secondary combustion occurs at the exit of the radiant boiler.

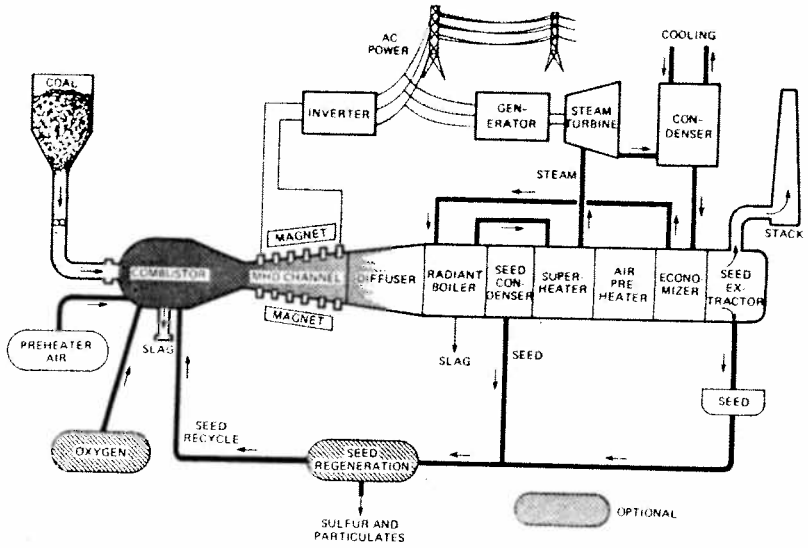

Fig. 6 OCMHD System

3.6.2 Electromagnetic Pumps

Electromagnetic (EM) pumps for liquid metals operate on the principle that the interaction between a magnetic field and an electrical current produces a body force in the fluid according to the familiar Lorentz Law. Practical electromagnetic pumps have been constructed on this principle for a wide range of pressure and flow combinations. The two basic categories are conduction and induction pumps. In a conduction pump, the current and magnetic field are supplied to the liquid metal by an external means (Fig. 1). Either direct or alternating currents (dc or ac) and fields may be used. In an induction pump, the current is induced within the liquid metal by an external traveling magnetic field (Fig. 4). Although within each category many variations are possible (Ref. 32,33), the two most-common EM pumps are the dc conduction pump and the ac linear induction pump.

The separately-excited dc conduction pump is the simplest EM pump. It consists of a liquid-metal-filled duct, usually rectangular, constructed of a high-strength, inert, non-magnetic material, such as stainless steel. The duct contains a pair of highly-conductive electrodes embedded in opposite sides that conduct current into and out of the fluid. A magnetic flux density $\vec{B}$ perpendicular to this current density $\vec{J}$ is produced externally, either by a separately-excited electromagnet or a permanent magnet. The interaction between $\vec{J}$ and $\vec{B}$ generates a body $\vec{J} \times \vec{B}$ force along the duct, thus providing the pumping force.

The higher efficiency of dc conduction pumps makes them more attractive than ac pumps. Some factors affecting the efficiency are the fluid and duct sidewall electrical conductivities, the cross-sectional and lengthwise aspect ratios, and the magnetic field gradients in the inlet and outlet regions of the pump. Efficiencies on the order of 70% have been measured, and predicted efficiencies on the order of 80% are attainable with insulating-sidewall ducts (Refs. 34-36). Though their input power characteristics require very high current at low voltage, the basic pumping force can be large. For example, with $J = 7.8\ MA/m^2$ and $B = 0.5$ T, an ideal pressure rise of 3.9 MPa per meter of pump duct length is obtained.

A large-scale application of a dc conduction pump would be as the primary pump in a liquid-metal-cooled fast breeder reactor. EM pumps offer significant advantages in the difficult reactor environment due to their inherent simplicity and lack of moving parts. EM pumps are particularly suited to the high flow, high head requirements of a primary pump. To overcome the need for an external high-current low-voltage supply, the dc pump can be directly

coupled with an MHD generator in a common magnetic field. In this device, intermediate loop liquid metal is forced through the generator section by the intermediate loop pump, generating a large direct current which is transferred to the pump section by short, low-resistance electrodes. The interaction of the current in the pump section with the external magnetic field produces flow in the primary loop. As shown in Fig. 7, the two flows are thus coupled together, and hence the device is referred to as a "flow coupler" (Refs. 36,37). The local generation of the current enables lower voltages and higher currents to be used than would be possible with an external supply. The lower voltages, in turn, reduce end current losses and permit higher overall efficiencies, on the order of 60%. Potentially the flow coupler could be integrated directly with the intermediate heat exchanger, allowing improved reactor layout and decreased containment size and cost.

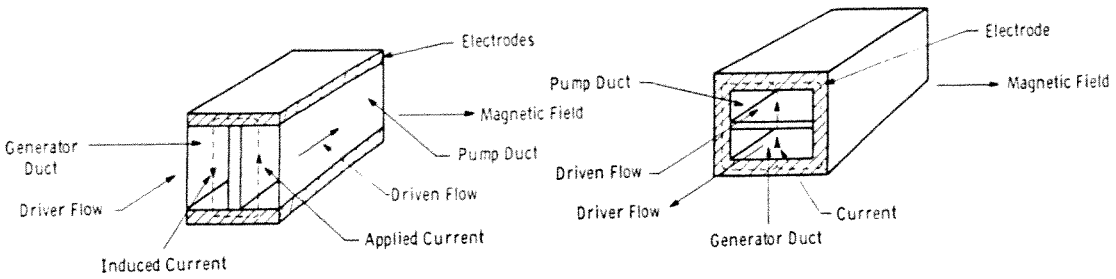

Fig. 7 Parallel and Anti-Parallel Flow Coupler Modules

AC induction pumps have been used since the 1950's (Refs. 32,33). There are linear (annular or flat) and helical versions, but above approximately 60 L/s, annular three-phase induction pumps are preferred (Ref. 38). In these pumps a travelling magnetic field sweeps the conducting fluid through a thin duct beneath the pole pieces. Efficiencies of over 40% have been predicted for large pumps at low pressure differences (less than 1.0 MPa). Forty-eight 30 L/s units have been in service at the Dounreay fast reactor (UK), representing a total operating experience of over two million hours, with only two failures, neither of which affected the fluid flow integrity. A 400 L/s unit has operated for over 60,000 hours on the EBR-II reactor at Arco, Idaho (U.S.) without failure.

A significant limitation on induction pumps is the attainable pressure difference. The fluid channel must be approximately one skin depth thick for reasonably efficient operation, and the duct walls must be much thinner (to minimize ohmic losses in the walls and distortion of the travelling magnetic field), so that structural considerations limit the operating pressure. Also, at very low flow rates these pumps are inferior to conduction pumps, since the separation between the pole teeth becomes impractically small for 50-60 Hz operation. In most cases of practical interest lower frequencies must be considered for induction pumps, and at the very low flow rates the advantages of induction pumps do not offset the disadvantage of the required frequency conversion equipment.

3.6.3 Heat Pipes

INTRODUCTION

A heat pipe is a high performance thermal transmission device that utilizes the latent heat of a working fluid to achieve energy transmission rates several orders of magnitude larger than that which can be transmitted in either a conventional convective flow system or a solid conductor of similar size. The full potential of heat pipes for high temperature applications was first demonstrated by Grover et al using sodium as the working fluid (Ref. 39). General background information pertaining to heat pipe theory and application is available through standard references (Refs. 40,41).

OPERATIONAL CHARACTERISTICS

A heat pipe basically is a closed tube or other structure containing a small amount of working fluid. In its simplest form, the heat pipe is a continuous two-phase heat transfer loop characterized by no moving mechanical parts, no auxiliary electric power requirements, and long life times. During operation, the working fluid is vaporized by heat input at the hot end or evaporator section, Fig. 8. The saturated vapor then flows down the core of the heat pipe (adiabatic section) to the cold end or condenser section, where it condenses releasing latent heat. In a conventional heat pipe, the condensate is returned through a wick structure to the evaporator section by capillary action and/or gravity. The term "heat

pipe" is also used to denote evaporation-condensation devices in which the condensate is returned by other means, such as magnetic volume forces or mechanical pumps. The central adiabatic section provides the physical connection between the hot and cold ends.

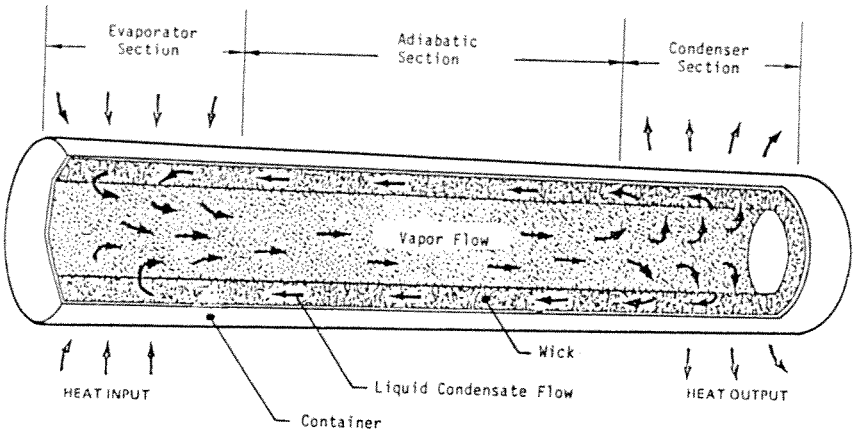

Fig. 8 Operation of a Basic Heat Pipe Element

The outermost shell or container is commonly a closed cylindrical tube for ease of manufacturing, but can be a square channel or practically any geometrical shape suitable for heat transfer. The wick structure is usually located adjacent to the container wall, and typically consists of several wrappings of wire mesh screen. Other wick structures include: porous sintered metal, axial groves on the inner wall of the container shell, tubular arteries, and composite materials. A high performance composite wick structure uses a layer of small pore size wire mesh or other material at the liquid-vapor interface to provide large capillary pumping forces, with axial groves or other large pore material in the annular region between the fine mesh and the container walls to give a low resistance flow path for the liquid condensate (Ref. 42).

Successful operation of heat pipes depends upon a continuous circulation of the working fluid, as vapor in the core and as condensate return in the wick. The circulation or axial heat transport capability of a heat pipe is limited by a number of physical processes (Refs. 40,43), classified as 1) viscous, 2) sonic, 3) entrainment, 4) wicking or capillary, and 5) boiling limits. The viscous limit occurs at low temperatures in relatively long heat pipes, when the axial heat flux is dominated by viscous pressure drop. The sonic limit occurs when the vapor exiting from the evaporator attains sonic velocity resulting in "choked flow". The entrainment limit occurs when the vapor velocity is high enough to shear and entrain liquid droplets from the condensate at the wick surface, resulting in insufficient condensate return to the evaporator. The wicking limit occurs when the pressure difference across the liquid-vapor interface at the wick surface is such that the liquid evaporates faster than it can be supplied by capillary pumping in the wick. The boiling limit occurs in the evaporator when condensate boiling takes place within the wick structure, forming vapor bubbles which interfere with the radial heat flux through the wick. The effects of these limitations are illustrated in Fig. 9. The actual shape of the operating area under the curve can vary significantly depending upon the wick structure, working fluid, and heat pipe geometric configuration. The heat transport capability for a given heat pipe is determined by which limitation has the lowest value at the temperature of interest.

HIGH TEMPERATURE APPLICATIONS

Heat pipe applications can be classified according to the temperature range of interest, and the appropriate working fluids for this range. Three logical categories are: 1) low-temperature or cryogenic, 2) moderate-temperature, and 3) high-temperature or alkali metal heat pipes. Only the later category is of interest here, and this includes applications beyond ~ 628 K since alkali metals boil at temperatures above this value at reasonable pressures. Sodium, lithium, and potassium have been used in the majority of alkali metal heat pipe applications to date, although other alkali metals have been used in laboratory investigations and for special applications.

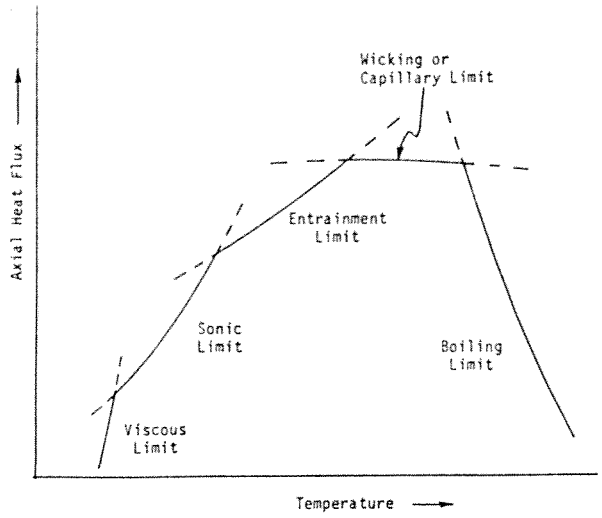

Fig. 9 Heat Transport Limitations for a Heat Pipe

Alkali metal heat pipes differ in several important characteristics from low and moderate temperature heat pipes:

1) The large surface tension coefficients correspond to good capillary pumping characteristics, and the wicking limit is generally not a problem.

2) The relatively low vapor density results in higher vapor velocities within the evaporator core, and the sonic limit is often a major constraint. The entrainment limit is also a major design factor due to high relative velocities across the liquid-vapor interface.

3) The working fluid is frozen for an initially ambient system, requiring special start-up procedures.

4) The large latent heat values yield much higher heat transport capabilities (typically, two or more orders of magnitude).

The corrosive nature of many alkali metals requires special attention to materials compatibility with the container and wick structure (Ref. 44).

Alkali metal heat pipes were originally developed for space power systems applications. They have been used in designing spacecraft radiators high temperature furnaces, nuclear reactor control systems, and other applications (Ref. 45). Considerable effort in recent years has been devoted to heat pipes for high-power-density thermionic converters, Fig. 10. A typical design might use silver or lithium heat pipes for transporting energy to the emitter, and sodium or potassium pipes for dissipating heat from the collector.

Heat pipes are ideal for integrating external combustion engines with remote heat sources. Stirling engines, for example, have been operated using sodium heat pipes as thermal flux transformers between the engine and combustion source (Ref. 46). A variety of design concepts for coal-fired Stirling engine power generation have been developed which require intermediate heat transport systems such as the pumped configuration shown in Fig. 11. Sodium heat pipes offer the best potential for integrating such engines with fluidized bed combustors (Ref. 47). Alkali metal heat pipes have also been used to integrate Brayton-cycle turbines with central solar receivers (Ref. 48), and in the development of high-temperature recuperators for industrial stack gases and other waste heat sources.

3.6.4 Thermionic Converters

INTRODUCTION

The thermionic energy converter, Fig. 12, converts heat directly to electricity without moving parts. As shown in Fig. 12, it consists of a hot electrode (the "emitter") facing a cooler electrode (the "collector") inside a sealed enclosure containing a controlled

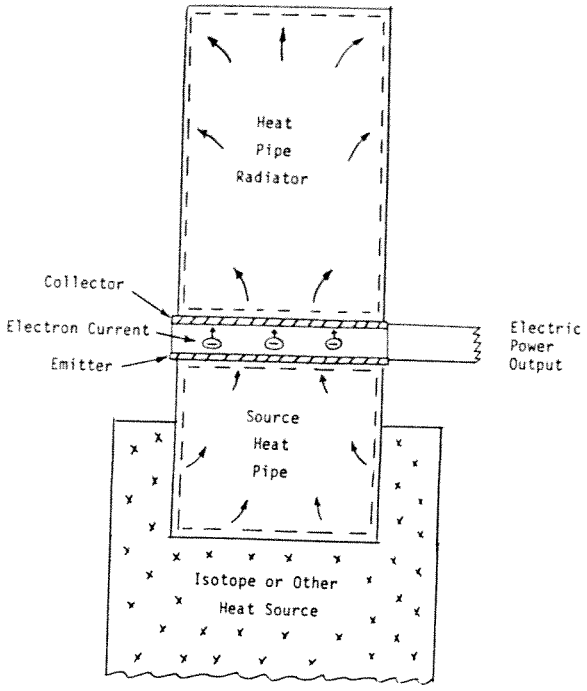

Fig. 10 Thermionic Converter Using Liquid Metal Heat Pipes

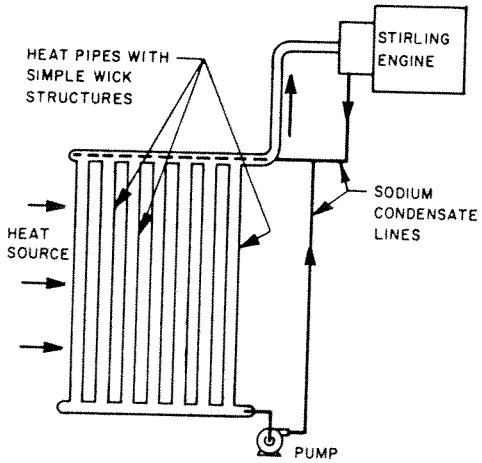

Fig. 11 Modified Heat Pipe System with Pump Assist

atmosphere. Electrons vaporized from the hot emitter move across the interelectrode space to the cooler electrode where they condense and then return to the emitter via the electrical load. In effect, the temperature difference between the emitter and collector drives the electrons through the load. Various geometries are possible, with electrodes arranged as parallel planes or as concentric cylinders. The space between the emitter and collector electrodes is typically less than three millimeters.

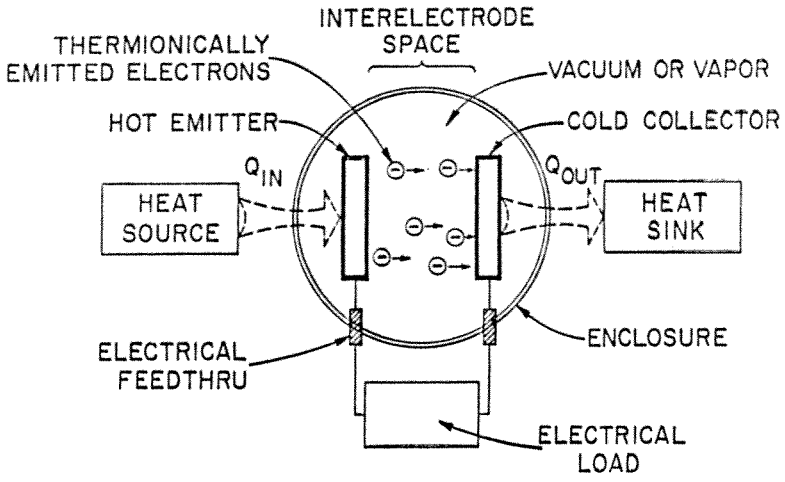

Fig. 12 Thermionic Converter Components

Thermionic conversion can be used with fossil fuel, solar, or nuclear energy sources. It is particularly attractive in combination with steam power plants, where part of the heat available at high temperatures can be converted into electricity thermionically before the balance of the heat is utilized in the steam plant at lower temperatures.

The principle of thermionic conversion is derived from Edison's discovery in 1885 that current could be made to flow between two electrodes at different temperatures in a vacuum (Ref. 49). The analysis and experimental investigation of thermionic emission from a hot electrode was performed by Richardson in 1912 (Ref. 50). Schlichter, in 1915, recognized this means of converting heat into electricity (Ref. 51). Langmuir and his associates theoretically and experimentally characterized the electron and ion emission from cesium adsorbed films on tungsten (Ref. 52). This work incorporated all the elements of what is now known as a cesium vapor thermionic converter. The first thermodynamic analysis of a thermionic converter, viewed as a heat engine operating across a temperature difference, was given by Hatsopoulos (Ref. 53). Further historical details are contained in Ref. 54.

BASIC PRINCIPLES

An idealized potential diagram of a thermionic energy converter is shown in Fig. 13. The diagram gives the spatial variation of the electrostatic potential perpendicular to the electrodes. Since the potential energy of the electrons in the collector is greater than that in the emitter, the collected electrons can perform work as they flow back to the emitter through the electrical load. The load voltage is given by the difference in the Fermi levels between the emitter and the collector. The Fermi level is the characteristic energy of a material under thermal equilibrium at which the probability of a quantum state being occupied by an electron is one-half. The difference between the Fermi level and the electrostatic potential at a surface is a property of the surface and is called the work function. The work function approximately equals the heat of vaporization of electrons. The emitter work function, ϕ_E, is given by the difference in potential of the emitter Fermi level and a point just outside the emitter. Likewise, the work function of the collector, ϕ_C is given by the potential difference between the collector Fermi level and a point just outside the collector. The current density of the thermionically emitted electrons is an exponential function of the ratio of the work function to the electrode temperature.

Space Charge

The negative space charge barrier is a consequence of the finite transmit time of the electrons crossing from the emitter to the collector. The electrons that are subsequently emitted are repelled by the electric field from the free negative electron charges and are reflected back to the emitter unless they have sufficient kinetic energy to overcome the repulsion and reach the collector.

There are three basic approaches to reducing the deleterious effects of space charge: 1) the close-spaced diode in which the interelectrode spacing is quite small, 2) ion additive

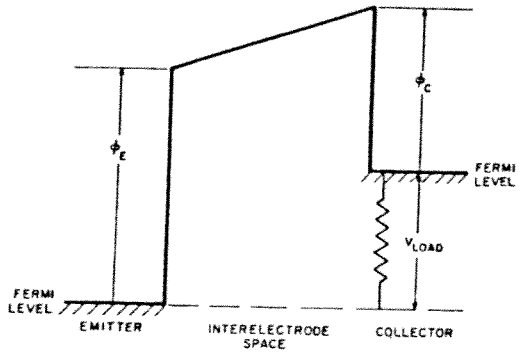

Fig. 13 Idealized Potential Diagram of Thermionic Converter

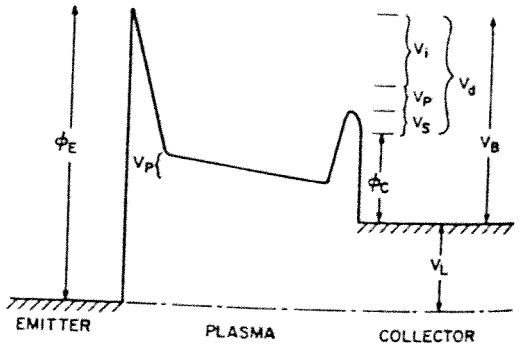

Fig. 14 Identification of Loss Mechanisms in the Thermoinic Diode

converters (e.g., surface contact ionization, "ignited" mode,hybrid mode, etc.) and 3) accelerating-decelerating converters (e.g., electrostatic triode and vacuum magnetic triode). Only the first two types of converters have generated electrical power at practical efficiencies.

In the vacuum diode, the space charge is suppressed by making the space very small (less than 25 micrometers). The practical difficulty of maintaining the necessary close spacing over large areas at high temperatures as well as the problem of maintaining a stable, low collector work function makes the vacuum diode mostly of academic interest.

The problems of extremely close spacing can be circumvented by introducing low pressure cesium vapor between the emitter and the collector (Ref. 55). This vapor is ionized when it contacts the hot emitter, provided the the emitter work function is comparable to the 3.89 eV ionization potential of cesium. Unfortunately, surface contact ionization is effective only when the emitter work function is high, which in turn necessitates impractically high temperatures.

To operate at more moderate temperatures, the cesium pressure has been increased by several orders of magnitude. Wilson (Ref. 56) proposed and demonstrated the usefulness of cesium adsorption on the emitter to reduce its work function so that higher current densities can be achieved at much lower temperatures than in the low pressure diode. Some of the emitted current is neutralized by thermionically emitted ions. This current corresponds to the "extinguished mode" part of the current-voltage characteristics. At lower load voltages the current increases substantially. At those voltages most of the ions for space charge neutralization are provided by electron impact ionization of the cesium in the interelectrode space. This part of the current-voltage characteristics is termed the "ignited mode". Sheath regions couple the emitter and collector to the interelectrode plasma where the ion and electron densities are roughly equal. Because cesium pressures of several torr are required to reduce the emitter work function to the desired level, the electrons are scattered many times by cesium atoms as they cross to the collector. This results in a resistive loss in the plasma, usually termed the "plasma drop". There are other losses due to ionization and the double sheath at the collector. The sum of the plasma, ionization and sheath potential losses is usually called the "arc drop" and is denoted on the potential diagrams as V_d. For high efficiency, it is clear that V_d and ϕ_C should be small.

Since the adsorbed cesium layer greatly lowers the electrode work function, the high pressure cesium diode can operate at a substantially lower emitter temperature than the low pressure device. Typical operating temperatures of ~1900 K allow application to nuclear reactors for space power.

Barrier Index

The barrier index, V_B, is a parameter that serves as a figure-of-merit for characterizing thermionic converter performance. The lower the V_B, the higher the converter performance. Reductions in V_B can be translated into higher efficiency at a given temperature or a lower emitter temperature at a given efficiency. Operationally, V_B is defined as the potential difference between the tangent to the measured current-voltage characteristic and the tangent to the Boltzmann line. (The ideal current-voltage characteristic assuming zero arc drop, zero collector work function and zero collector temperature). Within terms of the order of 0.1 eV, the components making up the barrier index are illustrated in Fig. 14. The

barrier index, V_B, is the sum of arc voltage drop, V_d, and the collector work function, ϕ_c. The arc drop is composed of three elements: 1) plasma loss, V_p, due to electron scattering by collision with the cesium atoms, 2) sheath loss, V_s, caused by the double-valued potential sheath adjacent to the collector and 3) ionization loss, V_I, associated with the ionization of cesium atoms by electrons. Typically, V_I, is about 0.4 eV.

APPLICATIONS

Thermionic conversion is one of the most attractive options for use with space reactors (Refs. 57, 58, 59). The mechanical simplicity associated with no moving parts implies reliability. The high temperature of heat rejection minimizes the mass of the radiator,which is usually the heaviest component of large space power systems. The high heat rejection temperature also limits the size of the radiator, which is an important consideration, since all (United States) space reactor systems in the foreseeable future must fit inside the space shuttle bay. Modularity maximizes reliability by eliminating single point system failures. Although thermionic efficiencies up to 15 percent have been demonstrated; higher efficiencies are theoretically possible with reduced electrode and plasma losses. In addition, thermionics is a demonstrated conversion technology coupled to nuclear reactors (Refs. 60, 61).

Two basic system approaches have been pursued for thermionic reactors, in-core and out-of-core. The former approach, which incorporates the converters inside the core, is illustrated in Fig. 15a. This in-core design concept has been utilized in the TOPAZ reactor (Refs. 60,61) and in in-pile tests conducted in the United States in the sixties and early seventies. The out-of-core system, Fig. 15b, transfers the thermal energy outside the reactor to a bank of thermionic converters. For a given power level, the reactor and shield have a lower mass and the conversion system is decoupled, to a large extent, from the reactor. In addition, mechanical coolant pumping is eliminated and heat pipes lend themselves to redundant systems.

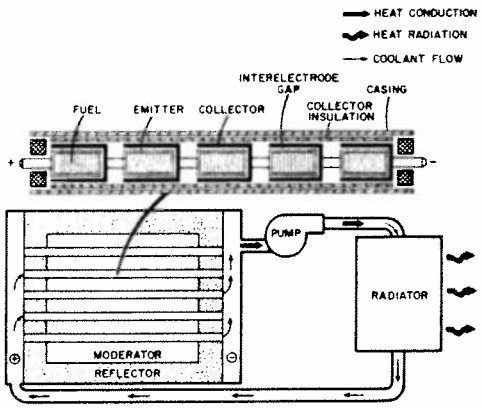

Fig. 15a In-Core

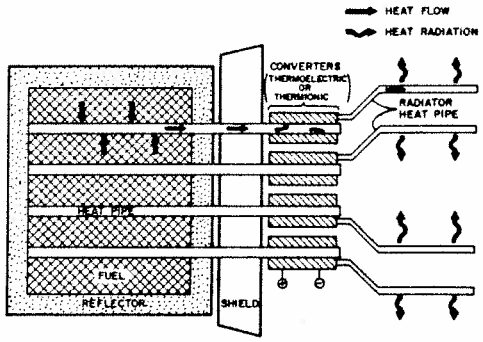

Fig. 15b Out-of-Core

Fig. 15 Thermionic Reactor Concepts

The thermionic technology, developed for space has provided the basis for terrestrial applications. The high emitter temperatures necessary for efficient operation, typically > 1600 K, require refractory metals which must be protected from air for non-space applications. The thermionic converter illustrated in Fig. 16 is representative of the combustion-heated diodes that have been constructed and tested (Ref. 62). The torispherical dome, which is the active area of the converter, is exposed to high-temperature combustion. Electrons evaporated from the tungsten emitter are condensed on the mating nickel collector which is air cooled. A ceramic seal provides electrical insulation between the electrodes. A typical output potential is half a volt at current densities between 5 and 10 A/cm^2. The ceramic spacer establishes the spacing between the emitter and collector.

Terrestrial applications of interest include powerplant topping and cogeneration. Previous studies of topping central station powerplants (Refs. 63,64) with thermionics have projected that fully developed thermionic energy converters could add as much as 10 percentage points to their overall efficiency. Investigation of topping gas turbine plants with thermionic converters (Refs. 65,66) have suggested that efficiency gains of around 2.5 percent could be

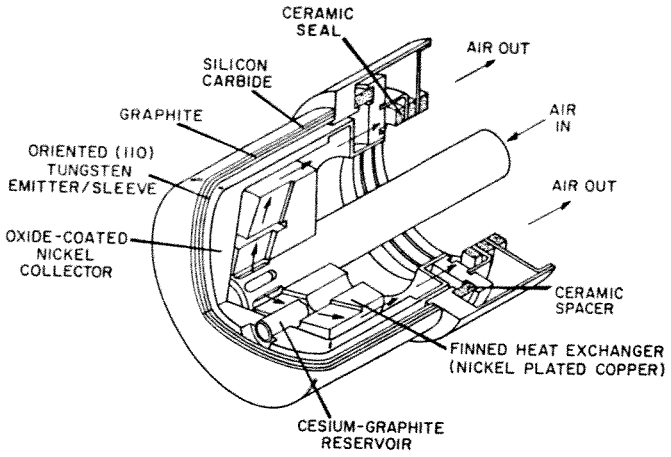

Fig. 16 Combustion-Heated Thermionic Converter

obtained using persent converter performance. Less detailed estimates have indicated that state-of-the-art converters could provide 4 to 5 percentage points of efficiency to central station efficiency. These studies also show that the installed cost of thermionic converters in these systems is around 600 $/kWe.

A characteristic of thermionic converters is that the temperature of the heat rejected from the collector of the thermionic converter is high enough to generate steam without shifting the operating point of the Rankine cycle. This feature provides the distinct possibility of retrofitting existing utility plants to provide both increased efficiency and capacity.

Thermionic converters are also well adapted to cogeneration with high-temperature processes which require direct heating. It is one of the few conversion techniques that operate at a high enough temperature to permit the use of cogeneration with direct heating applications. A diagram illustrating the thermionic cogeneration burner module concept is shown in Figure 17. The combustor wall is lined with thermionic converters. The emitters of the converters receive energy from the combustion gases and convert part of this energy to electricity while rejecting the balance of the collector where it is picked up by the air used for combustion. Although the thermionic diode efficiency is only about 12 percent, the effective cogeneration efficiency is around 85 percent. This high conversion efficiency makes thermionic cogeneration attractive from both fuel utilization and economic viewpoints, especially for high temperature processes (Ref. 62).

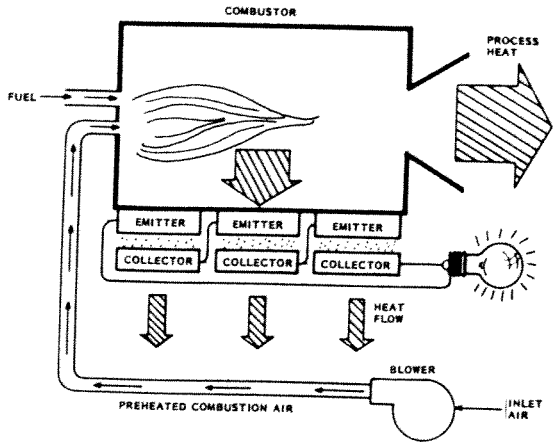

Fig. 17 Thermionic Cogeneration Burner Concept

REFERENCES

1. Sporn, P. and Kantrowitz, A., Power, 103 (1959).
2. Proc. 21st Symp. Eng. Aspects of MHD, Argonne Nat. Lab., Argonne, IL, (1983).
3. Proc. 7th Intnl. Conf. on MHD Elec. Power Generation, Boston, MA, (1980).
4. Petrick, M. and Shumyatsky, B. Ya, eds., Open-Cycle Magnetohydrodynamic Electrical Power Generation, Argonne National Laboratory (1978).
5. Reed, C. B., Proc. Rand Corp. Conf. on Liquid-Metal MHD Power Generation, R-2290-DOE, Rand Corp., Santa Monica, CA, 61-74 (1978).
6. Amend, W. E., and Petrick, M., Proc. 5th Intnl. Conf. on MHD Elec. Power Generation, Munich, Germany, Vol. IV, 125-140 (1971).
7. Pierson, E. S., Proc. 16th Intersociety Energy Conversion Engineering Conf., Atlanta, GA, 1525-1530 (1981).
8. Pierson, E. S., "Liquid-Metal MHD for Space Power Systems, "Proc. Special Conf. on Prime Power for High-Energy Space Systems, Norfolk, VA, (1982).
9. Petrick, M., and Roberts, J. J., Electricity from MHD, Warsaw, Poland, 1501-1520 (1968).
10. Hsu, C., Petrick, M., and Pierson, E. S., Proc. 5th Intnl. Conf. on MHD Elec. Power Generation, Munich, Germany, 63-79, (1971).
11. Gherson, P., Lykoudis, P. S., and Lynch, R., E., Proc. 7th Intnl. Conf. on MHD Elec. Power Generation, Cambridge, MA, 590-594 (1980).
12. Lykoudis, P. S., MHD-flows and Turbulence - II, Proc. 2nd Bat-Sheva Seminar on MHD Flows and Turbulence, Beer-Sheva, Israel, 183-192 (1978).
13. Fabris, G., Pierson, E. S., Pollack, I., Dauzvardis, P. V., and Ellis, W., Proc. 18th Symp. Eng. Aspects of MHD, Butte, M, (1979).
14. Branover, H., El-Boher, A., Hoch, E., Unger, Y., Yakhot, A., and Ailberman, I., "Hydrodynamic Investigation of Single and Two-phase Flow in Liquid-metal MHD Generator Channels," Annual Report, Mechanical Engineering Department, Ben-Gurion University of the Negev, Beer-Sheva, Israel (1979).
15. Tanatsugu, N., Fujii-E, Y., and Suita, T., J. Nuclear Science and Technology, 9, 753-5, (1972)
16. Saito, M., Inoue, S., and Fujii-E, Y., J. Nuclear Science and Technology, 15, 476-489 (1978).
17. Fabris, G., Chow, J. C. F., and Dunn, P. F., J. Power Engineering, 102, 820-826 (1980).
18. Elliott, D. G. and Weinberg, E., TR32-987, Jet Propulsion Laboratory, Pasadena, CA, (1968).
19. Liquid-metal Magnetohydrodynamics Technology Transfer Study, Vol, II, Appendix C, 1200-59, Jet Propulsion Laboratory, Pasadena, CA, (1973).
20. Cerini, D. J., and Hays, L. G., Proc. 15th Intersociety Energy Conversion Engineering Conf., Seattle, WA, 788-797 (1980).
21. Pierson, E. S., Branover, H., Fabris, G., and Reed. C. B., Mech. Eng., 102, 32-37 (1980).
22. Thibault, J. P. Joussellin, F., and Alemany, A., Proc. 21st Symp. Eng. Aspects of MHD, Argonne, IL, (1983).
23. Branover, H., "Conversion of Solar Heat into Electricity by Means of Liquid-Metal MHD Systems," Ben-Gurion University of the Negev, Beer-Sheva, Israel (1981).
24. Pierson, E. S., and Herman, H., Proc. 3rd Beer-Sheva Seminar on MHD-Flows and Turbulence, Beer-Sheva, Israel (1981).
25. Jackson, W. D., and Pierson, E. S., I.E.E.E. Conference Report, Series No. 4, 38-42 (1962).
26. Huhns, T., and Pierson, E. S., Proc. 14th Symp. on Eng. Aspects of MHD, Univ. of Tennessee Space Institute, TN, VI.4.1-VI.4.6 (1974).
27. Bjerklie, J. W., and Powell, J. R., Jr., Electricity from MHD, Warsaw, Poland, 1647-1664 (1968).
28. Bushkatov, V. A., et al, Proc. 17th Symp. Eng. Aspects of MHD, Stanford, CA, H.8.1-H.8.7 (1978).
29. Woodson, H. H., Wilson, G. L., and Lewis, A. J., Proc. 3rd Symp. Eng. Aspects of MHD, Rochester, NY, (1962).
30. Electric Power Generation from Coal: An Introduction to Magnetohydro-dynamics, U. S. Dept. of Energy, Fossil Energy Programs, Division of Magnetohydrodynamics (1979).
31. Pei, R. Y., and Hess, R. W., "The Noble-Gas Closed-Cycle System of Magnetohydrodynamic Power Generation," R-2128-ERDA, Rand Corp., Santa Monica, CA, (1977).
32. Blake, L. R., Proc. Inst. Elec. Engrs. (London), 104A, 49-63 (1957).
33. Foust, O. J., Sodium-NaK Engineering Handbook, IV, Sodium Pumps, Valves, Piping, and Auxiliary Equipment, Gordon and Breach, New York (1972).
34. McNab, I. R., Alexion, C. C., Keeton, A. R., and Ciarell, P. A., Proc. 3rd Beer-Sheva Seminar on MHD-Flows and Turbulence, Beer-Sheva, Israel (1981).
35. Hughes, W. F., and McNab, I. R., ibid.
36. McNab, I. R. and Alexion, C. C., "High-Efficiency DC Electromagnetic Pumps and Flow Couplers for LMFBRs," EPRI Final Report NP-1656 (1981).
37. Davidson, D. F., Duncombe, E., and Thatcher, G., Nuclear Energy, 20, No. 1 (1981).
38. Cambillard, E. and Schwab, B., French Report CEA-R-2523 (1964).
39. Grover, G. M., Cotter, T. P. and Erickson, G. F., J. Appl. Physics, 35, 1990 (1964).
40. Chi, S. W., Heat Pipe Theory and Practice, McGraw-Hill Book Co. (1976).

41. Dunn. P. D., and Reay, D. A., Heat Pipes, Pergamon Press (1978).
42. Kemme, J. E., Keddy, E. S., and Phillips, J. R., 3rd Intnl. Heat Pipe Conf., Palo Alto, CA, 260 (1978).
43. Busse, C. A., Intnl. J. of Heat & Mass Transfer, 16, 169 (1973).
44. Tower, L. K., and Kaufman, W. B., 3rd Intnl. Heat Pipe Conf., Palo Alto, CA, 303 (1978).
45. Winter, E. R. F., and Barsch, W. O., Advances in Heat Transfer, Academic Press, 219 (1971).
46. Asselman, G. A. A., and Green, D. B., Philips Technical Review, 33, 138 (1973).
47. Uherka, K. L., Daley, J. G., Holtz, R. E., and Teagan, W. P., Proc. 14th Intersociety Energy Conversion Engineering Conf., Boston, MA, 1124 (1979).
48. Wolf, D. A., and Tarter, J. O., Proc. Intnl. Solar Energy Conf., Philadelphia, PA, 427 (1981).
49. Preece, W. H., F.R.S., Proc. Royal Society, London, 38, 219 (1885).
50. Richardson, O. W., Philosophical Magazine and Journal of Science, Series 6, Volume 23, 594-627 (1912).
51. Schlichter, W., Annalen der Physik, (4), 47, 573-640 (1915).
52. "The Collected Works of Irving Langmuir," Vols. 3 and 5, edited by G. Suits, Pergamon Press, New York, (1961).
53. Hatsopoulos, G. N., Ph.D. Dissertation, M. Eng. Dept., M.I.T., Cambridge, MA (1956).
54. Hatsopoulos, G. N., and Huffman, F. N., Proc. 105th Intersociety Energy Conversion Engineering Conf., 342-350 (1975).
55. Marchuk, P. M., Candidates Disseratation Institute Physics Academy Science Ukr, S.S.R. (1951) Proc. Inst. Phys. Acad. Sci. Ukr,S.S.R. 7,3 (1956).
56. Wilson, V. C., Bul. Ann. Phys. Soc., 3, Series II, 266 (1958); and Journal of Applied Physics, 30, No. 4, 475-481 (1959).
57. T. M. Hsieh and W. M. Phillips, "An Improved Thermionic Power Conversion System for Space Propulsion," 13th IECEC Conf. Proc., p. 1917 (1978).
58. Huffman, F., Reagan, P., Miskokyz, G., and Merrill, O., Proc. 17th Intersociety Energy Conversion Engineering Conf., 1908-1912, Los Angles, CA, 1908-1912 (1982).
59. Welch, J. R., Rasor, N. R., Britt, E. J., and Fitzpatrick, G. O., Proc. 18th Intersociety Energy Conversion Engineering Conf., Orlando, FL (1983).
60. V. A. Kuznetsov et al., Atomnava Energiva, 36, 450 (1974).
61. V. A. Kuznetsov, Proc. 11th Intersociety Energy Conversion Engineering Conf. (1976).
62. Huffman, F., Proc. 18th Intersociety Energy Conversion Engineering Conf., Orlando, FL (1983).
63. G. Miskolczy, B. Gunther and A. E. Margulies, "Conceptual Design of a Thermionic Topped Steam Electric Generator Plant Using an Advanced Boiler Concept," Proc. 13th IECEC, San Diego, p. 1893. (1978).
64. G. O. Fitzpatrick and E. J. Britt, "Increased Central Station Powerplant Efficiency with a Thermionic Topping System," Proc. 12th IECEC, p. 1602 (1977).
65. G. Miskolczy, C. C. Wang, D. Lieb, A. E. Margulies, L. J. Fusegni and B. J. Lovell, "Thermionic Combustor Application to Combined Gas and Steam Turbine Power Plants," Proc. 16th IECEC, Atlanta, p. 1956.
66. G. O. Fitzpartick, E. J. Britt, R. S. Dick, R. F. Lohneiss, R. A. Sederquist, "Thermionic Topping Systme for Increased Performance in Gas Turbine Powerplants," Proc. 16th IECEC, p. 1962 (1981).